Biology and Fertility of Soils (2023) 59:217–232
https://doi.org/10.1007/s00374-022-01690-5

ORIGINAL PAPER

Soil water extract and bacteriome determine N_2O emission potential in soils

Matthew P. Highton[1] · Lars R. Bakken[2] · Peter Dörsch[3] · Sven Tobias-Hunefeldt[1,4] · Lars Molstad[3,5] · Sergio E. Morales[1]

Received: 25 April 2022 / Revised: 5 December 2022 / Accepted: 7 December 2022 / Published online: 1 February 2023

Abstract

Soil chemical properties and microbiome composition impact N_2O emission potential, but the relative importance of these factors as determinants of N_2O emission in denitrifying systems is rarely tested. In addition, previous linkages between microbiome composition and N_2O emission potential rarely demonstrate causality. Here, we determined the relative impact of bacteriome composition (i.e., soil extracted bacterial cells) and soil water extract (i.e., water extractable chemicals and particles below 0.22 µm) on N_2O emission potential utilizing an anoxic cell-based assay system. Cells and water extract for assays were sourced from soils with contrasting N_2O/N_2O+N_2 ratios, combined in various combinations and denitrification gas production was measured in response to nitrate addition. Analysis of 16S amplicon sequencing data revealed similarity in composition between extracted and parent soil bacteriomes. Average directionless effects of cell and water extract on N_2O/N_2O+N_2 (Cell: Δ0.17, soil water extract: Δ0.22) and total N_2O hypothetically emitted (Cell: Δ2.62 µmol-N, soil water extract: Δ4.14 µmol-N) across two assays indicated water extract is the most important determinant of N_2O emissions. Independent pH differences of just 0.6 points impacted N_2O/N_2O+N_2 on par with independent water extract differences, supporting the dominance of this variable in previous studies. However, impacts on overall N_2O hypothetically emitted were smaller, suggesting that soil pH manipulation may not necessarily be a successful approach to mitigate emissions. In addition, we observed increased N_2O accumulation and emission potential at the end of incubations concomitant with predicted decreases in carbon (C) availability, suggesting that C limitation increases N_2O emission transiently with the magnitude of emission dependent on both chemical and bacteriome controls.

Keywords Denitrification · Greenhouse gases · Soil emission potential · Amplicon sequence variant · Bacteriome

✉ Matthew P. Highton
matthew.highton@gmail.com

✉ Sergio E. Morales
sergio.morales@otago.ac.nz

[1] Department of Microbiology and Immunology, University of Otago, 720 Cumberland Street, North Dunedin, Dunedin 9054, New Zealand

[2] Faculty of Chemistry, Biotechnology and Food Science, Norwegian University of Life Sciences, Ås, Norway

[3] Faculty of Environmental Sciences and Natural Resource Management, Norwegian University of Life Sciences, Ås, Norway

[4] Department of Experimental Limnology, Leibniz Institute of Freshwater Ecology and Inland Fisheries, Stechlin, Germany

[5] Faculty of Science and Technology, Norwegian University of Life Sciences, Ås, Norway

Introduction

Nitrous oxide (N_2O) is a potent greenhouse gas and ozone depleter accounting for around 6.2% of worldwide greenhouse gas emissions on a CO_2 mass equivalence basis (Intergovernmental Panel on Climate Change 2013). Around 45%of this is anthropogenically produced, mostly (60%) in agricultural settings via soil-based N transformations (Syakila and Kroeze 2011). Denitrification, the anaerobic microbial reduction of N compounds ($NO_3^- \rightarrow NO_2^- \rightarrow NO \rightarrow N_2O \rightarrow N_2$), is considered a major pathway of anthropogenic N_2O production (Bouwman et al. 2013). Soil conditions (e.g., O_2 concentration (Firestone et al. 1979; Smith and Tiedje 1979; Zumft 1997) and pH (Čuhel and Šimek 2011; Liu et al. 2014: Šimek and Cooper 2002)) can affect the ratio of the major gaseous end products of this process (N_2O and N_2) and overall process rates

resulting in higher or lower N_2O emissions to the atmosphere. Therefore, understanding the soil factors that favor low N_2O emission in the presence of available soil N is of great importance to manipulating agricultural systems towards reduced N_2O production in the future.

Conceptually, factors affecting soil N_2O emission potential can be separated into three categories: distal controls which act in the long term to determine denitrifier microbiome composition, the genetic and regulatory potential of the microbiome itself, and the immediate scale impact of proximal controls which may be transduced through the present denitrifiers (Wallenstein et al. 2006). Proximal factors such as O_2, pH, and temperature are easily isolated as independent variables, making them ideal experimental targets. In contrast, it is difficult to isolate microbiome impacts due to confounding by soil chemical and physical properties, likely distal controls. As such, microbiome-mediated effects are poorly understood. Studies are often theoretical (Graf et al. 2014) or correlative (Čuhel et al. 2010; Jones et al. 2014; Morales et al. 2010; Philippot et al. 2009; Samad et al. 2016), and it is often unclear whether the microbiome features described are the true drivers of an N_2O emission outcome. The issue is exacerbated when co-variance is observed with variables such as pH, which are known to affect both N_2O/N_2 emission ratios and changes in microbiome composition (Philippot et al. 2009; Samad et al. 2016).

Attempts have been made to control "all" variables relevant to denitrification within soils to isolate microbiome-based effects. However, this may not account for the effect of physical soil differences and certainly doesn't for unknown variables that may impact denitrification gas kinetics during experimentation (Cavigelli and Robertson 2000; Holtan-Hartwig et al. 2000). A solution to minimize such problems may be the extraction of whole soil bacteriomes. Though probably biased in the portion of soil communities extracted (e.g., Holmsgaard et al. 2011; Nadeem et al. 2013), this method has demonstrated that communities from different soils or the same soil under different long-term pH treatments will show contrasting N_2O emission responses to the same pH conditions (Dörsch et al. 2012; Liu et al. 2014).

Despite an increasing focus on microbiome impacts, the relative impact of proximal effects vs. microbiome composition on N_2O emission from denitrification is still poorly understood. In practice, should soil management be targeted towards proximal effects to control N_2O emissions, or is the long-term selection of certain denitrifier community biomes (distal control) more important?

Here, we incubated soil extracted cells in water extracts from pairs of soils with contrasting N_2O/N_2O+N_2 emission ratios in all combinations with the aim of identifying whether bacteriome composition (extracted cell origin) or proximal control (extracted chemical environment + particles under 0.22 µm) was the most important determinant of the contrasting N_2O/N_2O+N_2 ratios and total N_2O emission in our model system and soils in general. Assuming N_2O emission potential was rooted in extractable taxonomic and chemical properties of the tested soils, we hypothesized components from "high and low N_2O emitting" soils would respectively raise and lower N_2O/N_2O+N_2 emission ratios and total emissions in constructed assays. Further, we hypothesized that chemical differences (especially pH) would be the dominant effector while bacteriome composition effects would be weaker but still detectable. Analyses focused on the bacteriome as the extraction procedures have been developed around collection of bacterial cells (Lindahl and Bakken 1995). Soil cell extraction allowed treatment of bacterial communities as independent transferable units while soil water extracts ensured that whatever water-extractable components of the soil were present (e.g., dissolved C) reflected the parent soil in the produced incubation media. This is in contrast to traditional lab-based analyses which typically use a single simple C source.

Materials and methods

Soil sampling

Six soils were re-sampled from New Zealand South Island pasture farms previously sampled in Highton et al. (2020) (Karangarua, Makarora, Tapawera, Fairlie-Geraldine, Woodend, Rae's Junction). Sampling took place from 21st to 23rd of March, 2018. Soils were selected based on contrasting pH and N_2O hypothetically emitted (%) identified in Highton et al. (2020). Multiple soil cores (10 cm length, 2.5 cm diameter) were sampled along a 7.5 m transect evenly at distances of 0, 2.5, 5, and 7.5 m using a foot-operated auger until ~ 3 kg of soil was collected. Repeated cores at each distance were carried out in 4 perpendicular rows up to 6 cores across. Pooled site cores were stored field moist on ice in partially open ziplock bags during transport and at 4 °C in the lab. Grass, insects, worms and large roots were removed and cores were sieved at 2 mm. Sieved soils were stirred rigorously with a metal spoon to homogenize. Soils underwent a 36-h period without temperature control during transport to the Norwegian University of Life Sciences (NMBU, Ås, Akershus, Norway).

Soil pH

Soil pH was measured using both $CaCl_2$ (10 mM) and ddH_2O extractants as in Highton et al. (2020). Values were measured using an Orion 2 star pH meter (ThermoFisher Scientific, Waltham, MA, USA) with an Orion Ross Sure Flow Electrode (ThermoFisher Scientific), allowing up to 5 min for readings to stabilize.

Anoxic soil incubations

Anoxic soil incubations were carried out to determine denitrification gas kinetics and N_2O emission potentials. Incubations were prepared as in Highton et al. (2020) excluding overnight storage and oxic preincubation. Briefly, 3 mM NH_4NO_3 was amended to soils by a flooding and draining procedure to a moisture weight of 43 to 61%. Twenty grams dry weight equivalent of soil were weighed into triplicate 120 ml serum vials per soil. Vials were crimp sealed with butyl rubber septa and made anoxic by repeated evacuation and helium flushing.

Soil vials were incubated at 20 °C in a temperature-controlled water bath. Headspace gases (1 ml) were sampled every 4 h via an automated robotic gas sampling system (Molstad et al. 2007, 2016). Gases (O_2, CO_2, NO, N_2O, and N_2) were quantified in real time using a coupled Agilent 7890A gas chromatograph (GC) equipped with an ECD, TCD, FID, and chemiluminescence NOx analyzer (Model 200A, Advanced Pollution Instrumentation, San Diego, USA). An equal volume of helium is returned to the vials by back pumping ensuring consistent vial pressure. Dilution of headspace gases is accounted for later through back calculation. Gas concentrations were calibrated using certified standard gases supplied by AGA industrial gases (Oslo, Akershus, Norway). The overall system and its improvements are described in detail in Molstad et al. (2007, 2016).

Cell-based assay (CBA-int)

A soil extracted cell-based assay (CBA) was developed to determine the relative importance of bacteriome composition and soil chemistry on N_2O emission potential (see the "N_2O emission potential" section for metrics). Soil water extract (including particles below 0.22 µm) and cells were extracted separately from soils with similar native pH and contrasting N_2O ratios: Karangarua, a low N_2O emitting soil (N_2O ratio = 0.26, pH = 5.75) and Rae's Junction, a high N_2O emitting soil (N_2O ratio = 0.92, pH = 5.6). Separate extraction of soil cells and water extracts allowed them to be combined independently with components from alternate soils. Four possible combinations were produced to give the standard treatments: high emitting cells (HEC) + high emitting extract (HEE), high emitting cells (HEC) + low emitting extract (LEE), low emitting cells (LEC) + high emitting extract (HEE), low emitting cells (LEC) + low emitting extract (LEE). Standard treatments were carried out in triplicate vials. A minimum of duplicate 3 mM glutamate-amended controls of each treatment were produced to understand the impact of C limitation. Duplicate control incubations containing just extracted cells and milliQ were prepared to test the baseline activity of extracted cells. Occasional replication in duplicate was necessitated by limited vial space in the automated incubator/gas sampler. Cell negative controls were prepared to confirm the sterility of water extracts and to quantify the elution of any N_2 and O_2 remaining in the extract media after He flushing. Full treatment contents and replication is detailed in Table S1. Hereafter, this initial cell-based assay is referred to as CBA-int to differentiate it from the CBA using alternate pH soils (see the "Cell-based assay with alternate pH soils (CBA-pH)" section).

Water extract media preparation

Water extractable organic C (WEOC) extraction was prepared as reported by Guigue et al. (2014). Air-dried soil was combined with milliQ H_2O at a 1:3 ratio (170 g:510 ml) in 1 l Schott bottles. Bottles were shaken lengthways on an orbital shaker at 120 rpm for 1 h. Coarse particles were allowed to settle out for 5 min, and supernatant was poured into 250 ml polycarbonate Nalgene centrifuge tubes (ThermoFisher). Fine particles were removed by successive centrifugation (pelleting) and filtration steps: centrifugation at 4600G for 20 min using JXN-26 high-speed centrifuge with JS-7.5 swing out rotor (Beckman Coulter, Brea, CA, USA), filtration using 500 ml Sterafil Filter Holders (Merck, Burlington, MA, USA) loaded with 1.2 µm glass-fiber prefilters (Merck), and 0.45 µm cellulose filters (Merck) and syringe filtration using sterile 0.22 µm mixed cellulose ester filters (Merck). Filter sterilized Na-glutamate solution was added to a portion of the water extract from each soil to give a final concentration of 3 mM. An equivalent volume of milliQ H_2O was added to the rest of the extract to account for dilution. Standard extracts, glutamate-amended extracts, and milliQ for C free controls were buffered to pH 6 using 20 mM Na-phosphate buffer, as this was the closest value to the parent soil pH_{H2O} (Rae's Junction = 5.60, Karangarua = 5.75) within the bufferable range. Extracts and milliQ were re-filtered at 0.22 µm to ensure sterility after pH and C manipulation 22.5 ml of solution was added to autoclaved 120 ml glass serum vials containing magnetic stir bars. Vials were crimp sealed with butyl rubber septa + aluminum caps. Anoxia was induced through 8 repeated cycles of vacuum evacuation and helium filling with continuous magnetic stirring at 360 rpm. Vials were stored at 8 °C until inoculation and incubation.

Cell extraction by low-speed centrifugation

The cell extraction procedure was modified from Lindahl and Bakken (1995) with cell separation on the basis of sedimentation rate using low speed centrifugation. Cell extractions were performed on the same day they would be used, using optimized conditions determined in an earlier test extraction yielding approximate cell extraction efficiencies

for each soil (Tapawera = 9.4%, Karangarua = 5.5%, Rae's Junction = 3.3%). Twenty grams of field moist soil was blended with 200 ml of milliQ H_2O in a two-speed Waring blender (Waring, Stamford, Connecticut, USA) on high for 3×1 min with 5 min intermittent cooling on ice between each blending run. Coarse particles were allowed to settle for 5 min before supernatant was poured off into sterile falcon tubes up to the 35 ml mark (equivalent to 8 cm centrifugation distance). Tubes were centrifuged at 1000G for 10 min with 4 °C cooling on a benchtop Mega star 1.6R centrifuge with a TX-150 swing out rotor (VWR, Radnor, PA, USA) to sediment out noncellular debris. Cell containing supernatant was recovered into additional falcon tubes and centrifuged at 10,000G for 20 min with 4 °C cooling to pellet cells using an Avanti JXN-30 highspeed centrifuge with JA 14.50 fixed angle rotor (Beckman Coulter). Supernatant was removed without disturbing the cell pellet. Cells were washed/resuspended with 40 ml milliQ H_2O, re-pelleted and supernatant was removed. Cells were re-suspended and pooled to a final stock concentration of 6.25×10^8 cells ml^{-1} based on predictions from previously performed cell extraction and cell counts from the same soils.

Cell counts

Two milliliters of cell extract solution was collected for cell quantification at the time of initial blending and after washed cell re-suspension in milliQ H_2O. Samples were amended with gluteraldehyde to give a 1.5% fixation solution and stored at 4 °C for at least 2 h to allow fixation. Cell counts were carried out using SYBR Green staining and epifluorescence microscopy (Noble and Fuhrman 1998). Cell solutions were diluted 200-fold, and 6 ml was vacuum filtered through 0.2 µm Anodisc 25 diameter filters (Whatman, Maidstone, UK). SYBR Green I (Molecular Probes, Eugene, Oregon, TX) was diluted to a 2.5×10^{-3} working solution. Filters were placed on a 100 µl drop of solution and allowed to stain for 20 min in the dark. Filters were oven dried at 60 °C. Duplicate filters per sample were prepared. Filters were mounted onto glass slides with an antifade mounting solution consisting of 50% glycerol, 50% phosphate-buffered saline (0.05 M Na_2HPO_4, 0.85% NaCl, pH 7.5) and 0.1% p-phenylenediamine. Cells were counted by epifluorescence microscopy.

Inoculation and incubation

All vials used for incubation were placed in a 20 °C water bath. After temperature equilibration, headspace overpressure was removed by piercing the septa with a water filled syringe without plunger. All vials were amended with 0.5 ml He-flushed NH_4NO_3 solution to give a 3 mM final concentration. Two milliliters of helium-washed, concentrated cells from the appropriate soil were added to give a total of ~ 5×10^7 cells ml^{-1} in each standard, glutamate-amended, and C-negative treatment. Two milliliters of He flushed milliQ H_2O was added to make up the volume in cell-free water extract controls. Vials were magnetically stirred at 360 rpm. Headspace gases were sampled and measured every 4 h using the robotic autosampler gas chromatographs described above under anoxic soil incubations.

Cell-based assay with alternate pH soils (CBA-pH)

The cell-based assay experiment was repeated using soils with contrasting pH and N_2O ratios (see the "N_2O emission potential" section) to test the impact of cells and water extract within the context of added pH complexity (hereafter referred to as CBA-pH). Rae's Junction was used as a high N_2O-emitting, low pH (native pH = 5.60, N_2O ratio = 0.92) soil, as in CBA-int, while Tapawera was used as the higher pH low N_2O-emitting soil (native pH 6.58, N_2O ratio = 0.68). Again, Rae's Junction water extracts were buffered to pH 6. Tapawera water extracts were buffered closer to the native soil pH at 6.6. Triplicate standard treatments and their pHs were: HEC + HEE (6), HEC + LEE (6.6), LEC + HEE (6), LEC + LEE (6.6). Minimum duplicate alternative pH controls were produced for each treatment in which the pH of the treatment water extract media was switched to the opposite pH. This allowed us to determine the effects of pH and water extract independently from each other. Duplicate C-negative controls and cell-negative controls were set up as in CBA-int, but glutamate-amended treatments were not included. Full treatment contents and replication is detailed in Table S1.

Nitrate and nitrite quantification

Nitrate and nitrite ($NO_3^- + NO_2^-$) concentrations in soil water extracts were determined before using them as incubation media by a previously described chemiluminescent detection method (Braman and Hendrix 1989; Lim et al. 2018). This allowed accurate adjustment to 3 mM NO_3^- before use in the CBA. Ten microliters of water extract was injected into a reaction crucible. Signal peak areas were calibrated using 10 µl injections of a tenfold KNO_3 or KNO_2 dilution series (1 to 0.001 mM). A single replicate from each CBA treatment was sampled every ~ 24 h (0.15 ml) for immediate quantification of accumulated NO_2^-.

N_2O emission potential

N-gas kinetics recorded during incubation of soils and CBA treatments were used to evaluate N_2O emission potentials based on two time-integrated measures: hypothetically emitted N_2O (from here on referred to as N_2O emitted) and

its $N_2O/(N_2O+N_2)$ ratio (from here on referred to as N_2O ratio). Hypothetically emitted N_2O is calculated as the sum of net positive N_2O accumulations between each sampling point (i) over the course of the incubation accounting for N_2O lost by sampling (cumulative values, trapezoid integration). The max value for i was set at the point of consumption of all added N to N_2 (soils) or 22 sampling points for incubations that did not complete processing of added N (CBA). Hypothetical emissions refer to a conservative estimate of the N_2O that would escape to the atmosphere in an uncapped system. Let $\Delta N_2O_{(i)}$ denote the amounts of observed changes of N_2O in a flask between sampling point (i-1) and (i), plus the calculated sample loss at sampling point (i). We define N_2O hypothetically emitted between those sampling points to be $\max(0, \Delta N_2O_{(i)})$ (i.e., zero if $\Delta N_2O_{(i)}$ is negative, and $\Delta N_2O_{(i)}$ otherwise). Periods of net N_2O reconsumption from vial headspace are thus zeroed, as this would not occur in an uncapped system. For the whole experiment run,

$$N_2O \text{ hypothetically emitted} = \sum_{i=2}^{22} \max(0, \Delta N_2O_{(i)})$$

The $N_2O/(N_2O+N_2)$ ratio is calculated as N_2O hypothetically emitted over total N potentially emitted as N_2O. Total potential emissions are the sum of changes in accumulated N_2 and N_2O between each sampling point (i) over the course of the incubation, accounting for gases lost or gained by sampling and leakage (cumulative values, trapezoid integration). In short, the total gaseous N remaining at the end of the incubation. The present N_2O ratio formula generates a very similar value to the N_2O hypothetically emitted % value used previously in Highton et al. (2020) but may be applied where data has multiple N_2O production and consumption peaks over time and where processing of added N does not reach completion.

$$N_2O \text{ ratio} = N_2O \text{ hypothetically emitted} / \text{Total N potentially emitted as } N_2O$$

$$N_2O \text{ ratio} = \sum_{i=2}^{22} \max(0, \Delta N_2O_{(i)}) / \sum_{i=2}^{22} \left(\triangle N_{2(i)} + \triangle N_2O_{(i)} \right)$$

Differences in N_2O emitted and N_2O ratio between treatments were evaluated based on non-overlapping 95% confidence intervals. Specific comparisons between treatments were used to isolate either the effect of the extracted cells, the water extract or pH. For example, a comparison of the HE cells + HE extract treatment with the HE cells + LE extract treatment (an independent change of the water extract variable only), indicated an impact of water extract origin. Similarly, the comparison of the LE cells + LE extract treatment with the LE cells + HE extract treatment indicated the impact of water extract origin. Comparisons involved a directional element as HE chemical extracts, HE cells, and low pH were expected to increase emissions and LE treatments vice versa. Positive difference value were used to indicate that the HE treatments resulted in higher emissions metrics while a negative values denote lowered emissions metrics. When averaged, effects were maintained as positive or negative values unless stated that the effect size given was directionless (only magnitudes).

Estimated denitrification rates were calculated in the following manner. Estimated total denitrification rates excluded nitrate reduction.

$$\text{Estimated } N_2O \text{ reduction rate} = N_2 \text{ accumulation rate}$$

$$\text{Est NO reduction rate} = N_2O \text{ accumulation rate} + \text{Est } N_2O \text{ reduction rate}$$

$$\text{Est nitrite reduction rate} = \text{NO accumulation rate} + \text{Est NO reduction rate}$$

$$\text{Estimated total denitrification rate} = \text{Est } N_2O \text{ reduction rate} + \text{Est NO reduction rate} + \text{Est nitrite reduction rate}$$

Bacteriome composition

For each soil, DNA was extracted from extracted cell stock and parent soil to determine both cell extraction bias and community differences between separate cell extracts. For soils, parent soil was collected before the cell extraction protocol and stored at −80 °C until DNA extraction of duplicate 0.25 g replicates using the DNeasy powerlyzer powersoil extraction kit (Qiagen, Hilden, Germany). Duplicate 5 ml cell stock aliquots were harvested just prior to inoculation of cell-based assay treatments and frozen at −80 °C until cell pelleting and DNA extraction.

16S amplicon sequencing of samples was carried out on Illumina HiSeq using Version 4_13 of the Earth Microbiome Project standard protocol (Caporaso et al. 2012). Sequences are available in the NCBI Sequence Read Archive under BioProject ID PRJNA678002. Sequence quality control and ASV (Amplicon sequence variant) picking was carried out in R version 3.6.1 (R Core Team 2016) using the dada2 pipeline version 1.12.1 (Callahan et al. 2016). Taxonomy was assigned using the SILVA database (version 132) (Quast et al. 2013) and the RDP (Ribosomal Database Project) Bayesian classifier (Wang et al. 2007). Sample sequence reads were rarefied 10 times to a depth of 11,500 sequences using phyloseq package functions (McMurdie and Holmes 2013). Independent rarefactions were combined and normalized to the number of rarefactions. Fractional ASV counts were rounded to integers.

Beta diversity and ASV sharing

All beta diversity and ASV sharing plots were generated using ggplot2 version 3.2.1 (Ginestet 2011) and adjusted with the ggpubr (Kassambara 2020) and forcats (Wickham 2020) packages unless otherwise stated. The phyloseq package (McMurdie and Holmes 2013) was used to calculate and display community composition dissimilarity, the mean number of shared and unique ASVs, and the relative abundance of organisms at the phylum rank with the additional usage of the dplyr (Wickham et al. 2019) and Rmisc (Hope 2013) packages. Community composition dissimilarity patterns were confirmed using vegan package (Dixon 2003) ANOSIM and ADONIS tests.

The fold change of ASV abundance differences between extracted cells and soil samples, and its accompanying p value was generated with the use of the edgeR (Robinson et al. 2009) package to identify significantly changing ASVs with an exact test. p Values were adjusted based on Benjamini–Hochberg p value correction, and ASVs were only displayed if their false discovery rate (FDR) was below 0.1. ASV Genus taxonomy was only labelled if abundance differed more than fivefold with a p value $< 1 \times 10^{-4}$.

Results

Soil and cell-based incubations have distinct gas accumulation patterns, but relative emission potential is conserved

Denitrification gas (NO, N_2O, N_2) kinetics were compared between soil and cell-based incubations to determine whether the cell-based system accurately reproduced the trends observed using whole soils. Soil incubations (Fig. 1A, Fig. S1) displayed a monophasic N_2O accumulation and depletion curve. N_2O ratios were determined by

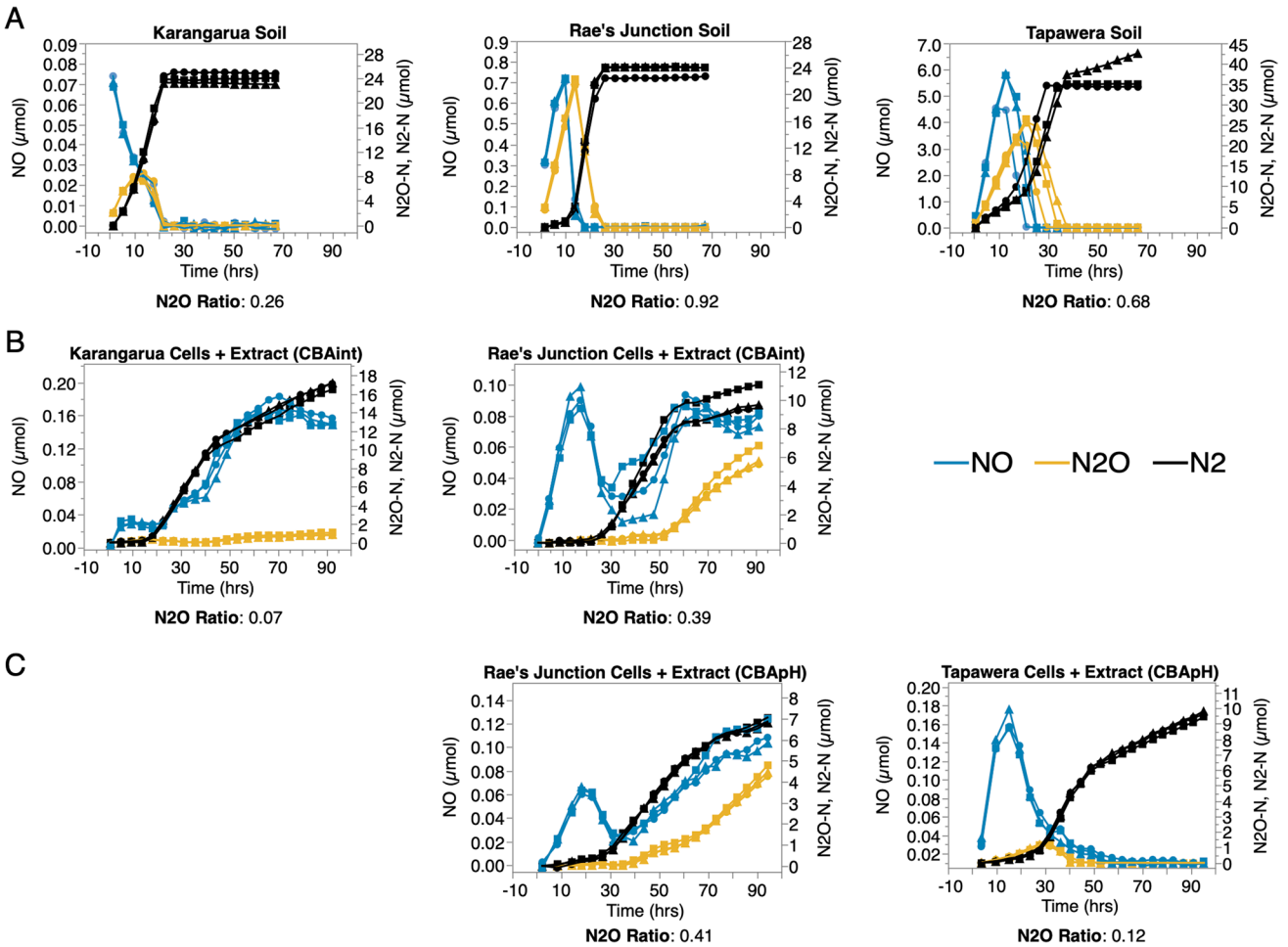

Fig. 1 Comparison of parent soils (**A**) and equivalent unswapped cell-based assay treatments (CBA) from CBA-int (**B**) and CBA-pH (**C**) reveal contrasting gas accumulation patterns. Headspace gases NO (blue), N_2O (orange), N_2 (black) were quantified every 4 h from triplicate (dots, squares, triangles) 3 mM NH_4NO_3-amended anoxic incubations. Note separate scales between treatments to highlight relative gas accumulation

the sequentiality of N_2O production and reduction steps as previously described in Highton et al. (2020). In the most extreme cases, close to all added N was accumulated as N_2O before high rate N_2 production/N_2O reduction was initiated, predicting high emissions from an in situ (unsealed) environment.

Gas accumulation patterns in cell-based incubations were somewhat distinct from soil incubations. Only + glutamate treatments of LE cells denitrified added N completely (Fig. S3B) during the experimental timeframe. Further, we noted 3 gas accumulation phases based on kinetics.

1) Lag phase: Most treatments experienced an initial lag phase in denitrification product accumulation and CO_2 accumulation (Fig. S2, Fig. S3, Fig. S4).
2) Low N_2O accumulation/complete denitrification: Following initial lag, early N_2O accumulation was very low and most gaseous N accumulated as N_2 (Fig. S3, Fig. S4).
3) High N_2O accumulation/incomplete denitrification: Major differences in N_2O accumulation, and thus N_2O ratio, occurred later in the incubation when estimated denitrification rates suddenly dropped, most notably N_2O reduction (N_2 production) (Fig. S2, Fig. S3, Fig. S4). Estimated N_2O production rates also dropped, but not significantly enough to prevent greater N_2O accumulation.

Despite distinct gas accumulation patterns, soil and cell-based assays sustained relative rankings based on N_2O ratios (Fig. 2, Rae's Junct > Tapawera > Karangarua). Gas production profiles were not completely consistent between separate cell-based assay runs as evidenced by the repeated Rae's Junction based incubations (Fig. 1, Rae's Junction CBA-int vs. Rae's Junction CBA-pH); however, this variation did not greatly impact N_2O ratios and relative ranking of incubations (Fig. 2).

Both soil water extract and bacteriome determine N_2O emission potential

We compared N_2O ratios and N_2O accumulation in a CBA (CBA-int) seeded with cells and water extracts from soils with similar native pH (5.6, 5.75) to determine whether bacteriome (cells) or chemical factors (extracts) were the most important determinant of N_2O emission potential in the absence of pH effects. Both cell and water extract origin affected N_2O ratio and N_2O emitted resulting in a gradient: HEC + HEE > LEC + HEE ≈ HEC + LEE > LEC + LEE (Fig. 3A, B). Cell and water extract origin had similar impacts on N_2O ratio but water extract origin was the most important determinant

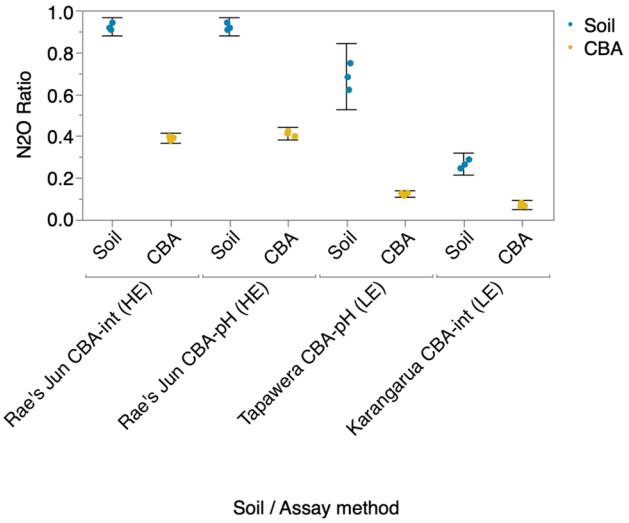

Fig. 2 Relative ranking of parent soil N_2O ratios is maintained in equivalent CBA treatments but lower on an absolute scale. N_2O ratios summarize the N_2O emission potential from 90-h CBA anoxic incubations amended with 3 mM NH_4NO_3 and are calculated as $N_2O/N_2O + N_2$ at the end of a CBA incubation, where periods of net negative N_2O accumulation are ignored to account for multiple gas peaks. Equivalent CBA treatments include both cells and water extracts derived from the parent soil. Results from triplicate vials per treatment are displayed with 95% confidence intervals

of overall emissions, with on average 60% greater impact (Table 1, CBA-int).

To account for the role of pH, soils with differing N_2O ratio and pH were also compared (CBA-pH). pH of the treatment was coupled to the soil water extract (HE extracts: 6.0, LE extracts: 6.6). Again, both cell and water extract origin (including coupled pH) affected N_2O ratio and N_2O emitted resulting in a gradient: LEC + HEE > HEC + HEE > HEC + LEE > LEC + LEE (Fig. 3C, D) but water extract origin was the most important determinant of both N_2O ratio and emissions (Table 1, CBA-pH). Patterns were largely determined by the unexpected emission patterns of LE cells which had very high emission potential in the presence of HE extracts yet low emission potential in the presence of LE extracts. Note, negative emission potential difference values (Table 1, CBA-pH) indicate the unexpected increase in emission potential using LE cells in the presence of HE extract.

pH has an outsized impact on low emitting cells

pH switched control treatments (HEE 6.0→6.6, LEE 6.6→6.0) revealed that the high N_2O ratio in the LEC + HEE treatment was largely a response to the low pH of the HE extracts; LE cell N_2O ratios were much more sensitive to independent pH change than HE cells (Table 2). We accounted for these strong impacts on LE cells by examination of the overall assay at pH 6.6,

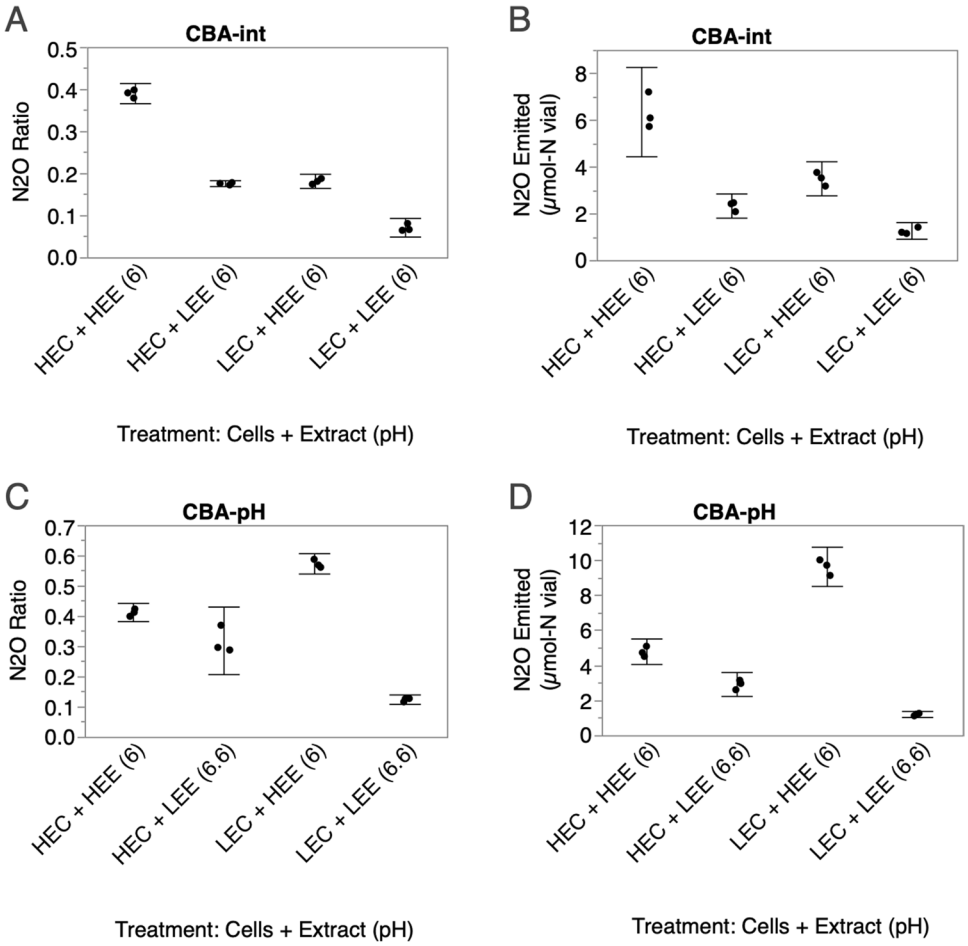

Fig. 3 Cell and water extract origin impact CBA N_2O ratios and N_2O emitted (µmol-N per vial). Standard swap treatments from CBA-int (**A**, **B**) or CBA-pH (**C**, **D**). N_2O ratios and N_2O emitted summarize the N_2O emission potential from 90-h CBA anoxic incubations amended with 3 mM NH_4NO_3 and are calculated as N_2O/N_2O+N_2 and total N_2O accumulated at the end of a CBA incubation, where periods of net negative N_2O accumulation are ignored to account for multiple gas peaks. Results from triplicate vials per treatment are displayed with 95% confidence intervals. pH of CBA-pH water extracts were buffered at two levels and are labeled accordingly

revealing a similar trend to the CBA-int assay: equal impact of cell and water extract origin on ratio (average change of 0.13 points), and greater impact of water extract on total N_2O emissions (average change cell = 0.37 µmol-N, water extract = 4.19, Table S2, overall). However, it should be noted that at pH 6.6, the HE extracts still lead to unexpectedly high absolute N_2O emissions from the LE + HE treatment due to the increase in total denitrification rate (Table S2, overall).

Comparison of independent pH, and water extract origin effects revealed two notable pH related phenomena:

1) Low pH drove large increases in N_2O ratio (average change 0.11 points), on par with independent water extract effects (Fig. 4A), yet only minor changes in total N_2O emissions (average 1.30 µmol-N, Fig. 4B) due to the contrasting impact of pH on total denitrification rates and N_2O ratios. In one instance pH increase to 6.6 actually increased total emissions (Table 2, 6 HEC + HEE).
2) Low pH and HE extract acted synergistically to increase LE cell emission potential, i.e., switching pH and water extract of the 6.6 LEC + LEE treatment to 6 and the HE extract (6.6 LEC + LEE vs. 6 LEC + HEE) lead to a greater increase in N_2O ratio and N_2O emitted than would be predicted by independent changes in pH or extract alone (Table 2). A much weaker positive synergistic effect (reduction in N_2O ratio and total N_2O) of LE extracts and LE pH (higher-6.6) on HE cells was also indicated (Table 2).

Carbon/starvation effect

We hypothesized that sudden changes in estimated denitrification rates (especially N_2 production) and emissions during the cell-based incubations were linked to shifts in C availability. + C (3 mM Na-glutamate) controls were included for each treatment in CBA-int to determine whether any of the observed differences in treatments were caused by changes in C availability. Divergence of gas accumulation rates in + C controls compared with standard treatments indicated that all CBA treatments became C limited during the incubation (Fig. 5). Further, C-amended controls did not experience the late incubation decreases in N_2 production rate, or the associated increased N_2O accumulation, seen in -C treatments. Estimated total denitrification rates and

Table 1 Differences in treatment N_2O ratio and N_2O emitted indicating strength of cell and water extract origin effects for CBA-int and CBA-pH

	CBA-int					CBA-pH			
Treatment	N_2O ratio	95% CI	N_2O emitted (μmol-N)	95% CI	Treatment	N_2O ratio	95% CI	N_2O emitted (μmol-N)	95% CI
HE cells + HE extract	0.39	0.37, 0.41	6.34	4.43, 8.25	HE cells + HE extract (6)	0.41	0.38, 0.44	4.77	4.04, 5.5
HE cells + LE extract	0.18	0.17, 0.18	2.32	1.8, 2.84	HE cells + LE extract (6.6)	0.32	0.21, 0.43	2.91	2.22, 3.58
LE cells + HE extract	0.18	0.16, 0.20	3.49	2.76, 4.22	LE cells + HE extract (6)	0.57	0.54, 0.61	9.61	8.49, 10.73
LE cells + LE extract	0.07	0.09, 0.10	1.25	0.9, 1.61	LE cells + LE extract (6.6)	0.12	0.11, 0.14	1.19	1.01, 1.36
Cell effect	Differences		Differences		Cell effect	Differences		Differences	
HEC + HEE vs LEC + HEE	0.21	0.19, 0.23	2.85	1.19, 4.52	HE, HE vs LE, HE	−0.16*	−0.19, −0.13	−4.85*	−5.77, −3.92
HEC + LEE vs LEC + LEE	0.10	0.08, 0.12	1.07*	0.64, 1.49	HE, LE vs LE, LE	0.19*	0.09, 0.3	1.72*	1.08, 2.35
Average cell effect	0.16		1.96		Average cell effect	0.02		−1.56	
Av directionless cell effect	0.16		1.96		Av directionless cell effect	0.18		3.28	
Extract effect	Differences		Differences		Extract effect	Differences		Differences	
HEC + HEE vs HEC + LEE	0.21	0.19, 0.24	4.02	2.26, 5.78	HE, HE vs HE, LE	0.09*	−0.01, 0.2	1.86*	1.22, 2.51
LEC + HEE vs LEC + LEE	0.11	0.09, 0.13	2.23*	1.62, 2.84	LE, HE vs LE, LE	0.45*	0.42, 0.48	8.43*	7.34, 9.51
Average extract effect	0.16		3.13		Average extract effect	0.27		5.14	
Av directionless extract effect	0.16		3.13		Av Directionless extract effect	0.27		5.14	

Emission metric differences are expressed relative to the HE extract or cells. Positive values indicate a reduction in the emission metric value when LE extracts or cells were used. Average cell effects are calculated using signed difference values while average directionless cell effects are calculated using absolute difference values

*Difference values have non overlapping confidence intervals with the appropriate comparison. Direct comparison of cell vs chemical extract difference values should be compared relative to the equivalent baseline treatment, i.e., HE, HE vs. LE, HE compared with HE, HE vs. HE, LE

Table 2 CBA-pH: difference in N_2O emitted and N_2O ratio associated with independent treatment difference in pH or water extract relative to a baseline sample

Baseline sample	Extract	95% CI	pH	95% CI	Extract + pH actual	95% CI	Extract + pH predicted (sum independent extract and pH differences)
Difference in N_2O ratio							
6 HEC + HEE	− 0.03	− 0.08, 0.01	− 0.03	− 0.33, 0.28	− 0.09	− 0.2, 0.01	− 0.06
6.6 HEC + LEE	0.07	− 0.21, 0.08	0.06	− 0.03, 0.15	0.09	− 0.01, 0.2	0.13
6 LEC + HEE	− 0.33	− 0.52, − 0.15	− 0.26	− 0.29, − 0.23	− 0.45	− 0.48, − 0.42	− 0.59
6.6 LEC + LEE	0.19	0.17, 0.21	0.12	− 0.13, 0.36	0.45	0.42, 0.48	0.31
Difference in N_2O emitted (μmol-N)							
6 HEC + HEE	− 1.74	− 2.52, − 0.96	0.98	− 2.31, 4.26	− 1.86	− 2.49, − 1.23	− 0.76
6.6 HEC + LEE	2.84	− 0.73, 6.4	0.12	− 0.88, 0.65	1.86	1.23, 2.49	2.96
6 LEC + HEE	− 7.17*	− 8.37, − 5.99	− 2.88*	− 3.85, − 1.93	− 8.42	− 9.51, − 7.34	− 10.06
6.6 LEC + LEE	5.54*	5.12, 5.96	1.25*	− 1.54, 4.04	8.42	7.34, 9.51	6.78

Negative values indicate a lower N2O ratio or hypothetical emissions relative to the baseline sample

*pH and extract difference values have non overlapping confidence intervals for equivalent baseline samples (same row)

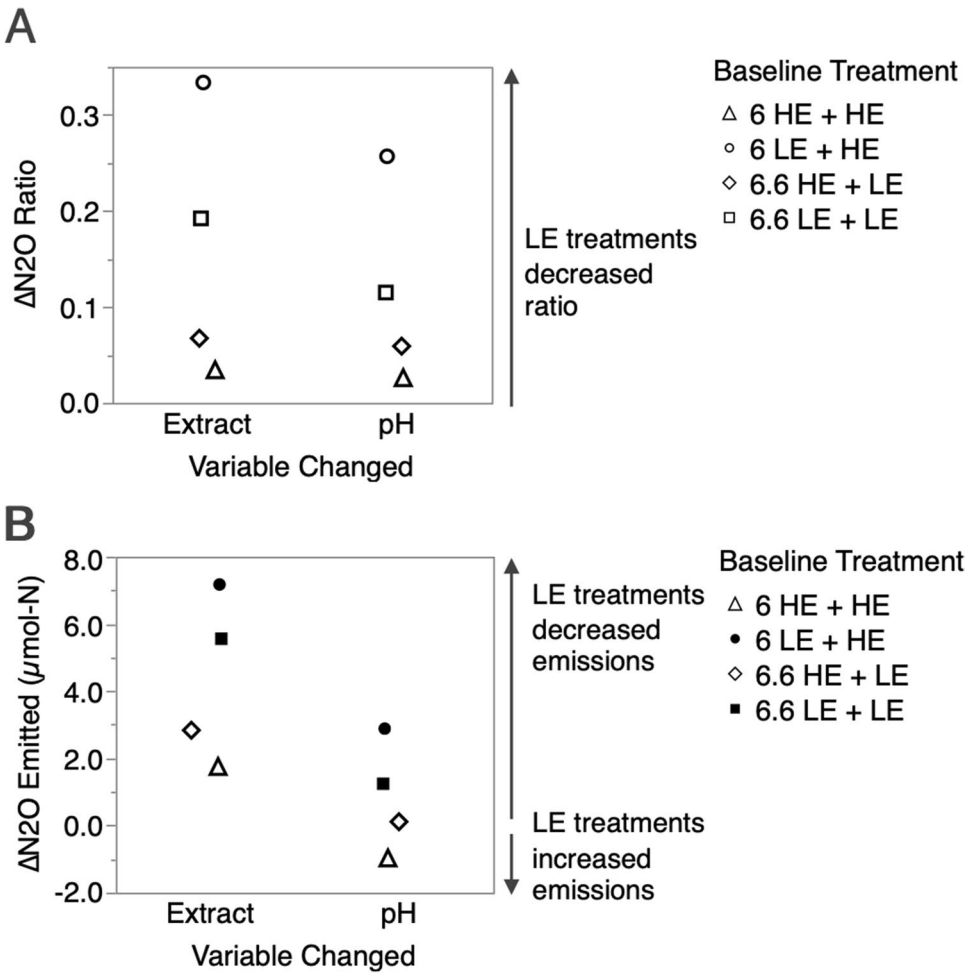

Fig. 4 Comparison of independent pH and water extract origin changes indicates similar impact of pH and water extract on N_2O ratios (**A**) but minor impact of pH on N_2O emitted (**B**). Each symbol compares the change in N_2O emission potential from 1 of 4 CBA-pH baseline treatments. Filled symbols indicate non-overlapping 95% confidence intervals for alternative pH or water extract changes to the same baseline treatment. Positive values indicate variable change had expected direction of effect on N_2O ratio or emissions, i.e., higher pH and LE extracts are expected to decrease N_2O ratio and emissions, lower pH, and HE extracts vice versa

CO_2 production rates typically dropped during the transition to the lower N_2 rate period also supporting increasing C limitation (Fig. S2). CO_2 rate drops during this time period were often well defined and of high magnitude but were less obvious for some incubations: HEC + LEE, 6 HEC + HEE, 6.6 LEC + LEE. We carried out a further analysis separating

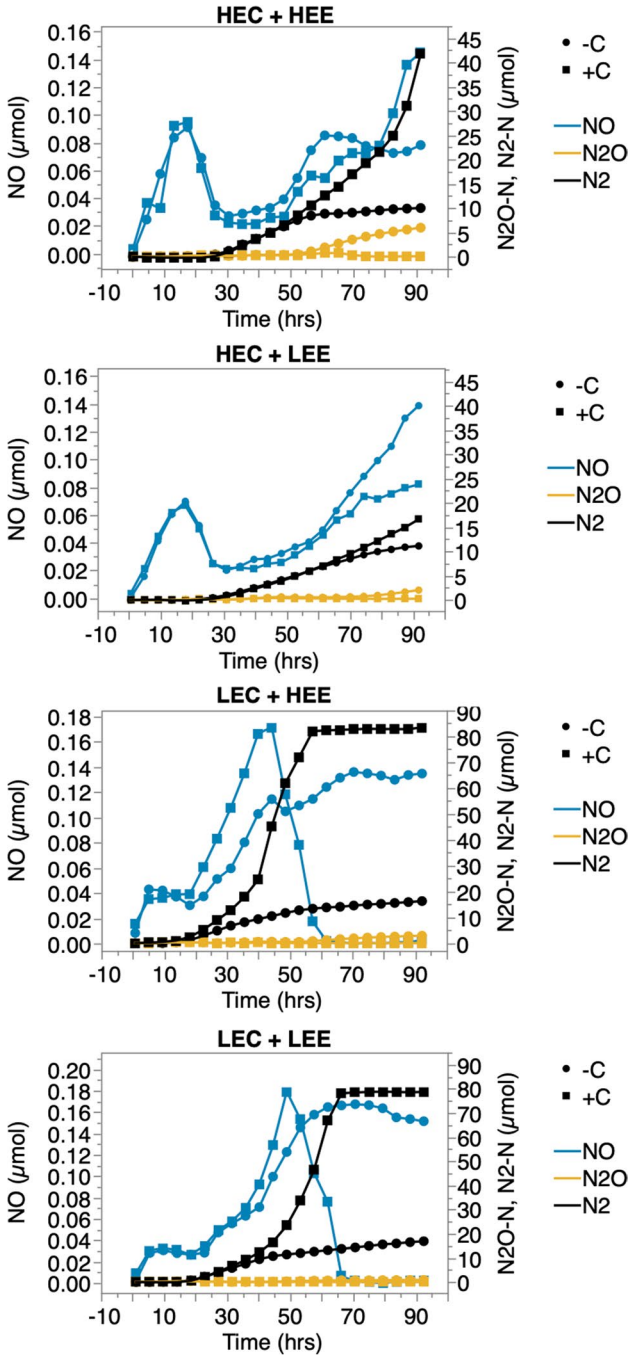

Fig. 5 Carbon limitation associated with increased N_2O accumulation and reduced N_2 accumulation in CBA-int incubations. Standard treatments (dots), 3 mM glutamate-amended treatments (squares). Headspace gases NO (blue), N_2O (orange), N_2 (black) were quantified every 4 h from 3 mM NH_4NO_3-amended anoxic extracted cell and water extract-based incubations. Average gas accumulation from triplicate (standard treatments) or minimum duplicate (glutamate amended treatments) vials per treatment are presented. Note separate scales between treatments to highlight relative gas accumulation

the impact of cell and water extracts during the C non-limited and limited periods of the incubation (Supplemental document S1, Fig. S5).

Bacteriome analysis

To assess if extracted cells were representative of soil bacteriomes, and to compare differences in bacteriomes across soils, we used 16S rRNA amplicon sequencing and processed results into amplicon sequence variants (ASVs). Bacteriome differences were primarily associated with soil origin (ANOSIM: $R^2 = 0.72$, $p < 0.001$, Fig. 6A) where extracted cells clustered alongside their original soils. However, small but significant changes were detected between extracted cells and soils (ANOSIM: $R^2 = 0.34$, $p = 0.003$). While both extracted cells and soils shared a large proportion (mean 50% with a standard deviation of 12%) of their total ASVs (Fig. 6B), extracted cells consistently recovered a larger number of ASVs (Wilcox, $W = 16$, $p = 0.029$). This bias in ASV detection was reflected at the phylum level (Fig. 6C) where Firmicutes were more represented in the soils compared to extract. It also highlighted differences between soils. To identify specific organisms with high or low relative extractability, differential abundance between soils and extracted cells were detected using an exact test (Fig. 6D). ASV's in the Bacillaceae family were significantly more abundant in soils relative to extracted cells but otherwise no consistent extraction bias was observed.

Discussion

Relevance of model to soils

The cell-based assay approach allowed causal linkage of bacteriome composition and soil water extractable components to N_2O emission potential. However, as with any model system, applicability to the initial environment studied is desirable. Conserved soil rankings based on N_2O ratios implied general relevance of the CBA system to soils (Fig. 2), however, several kinetic dissimilarities from soils resulted in different absolute N_2O ratios.

1) An initial lag phase in which cell-based assay incubations only accumulated very low concentrations of CO_2 and denitrification products NO_2^-, NO, N_2O, N_2 (Fig. S3, Fig. S4). This could hypothetically be caused by an initial lack of sufficient denitrifier cell density or a stress response to the cell extraction procedure. Lag or at least very low early denitrification activity and CO_2 production is also observable in some previous soil-extracted cell-based experiments, though the cause

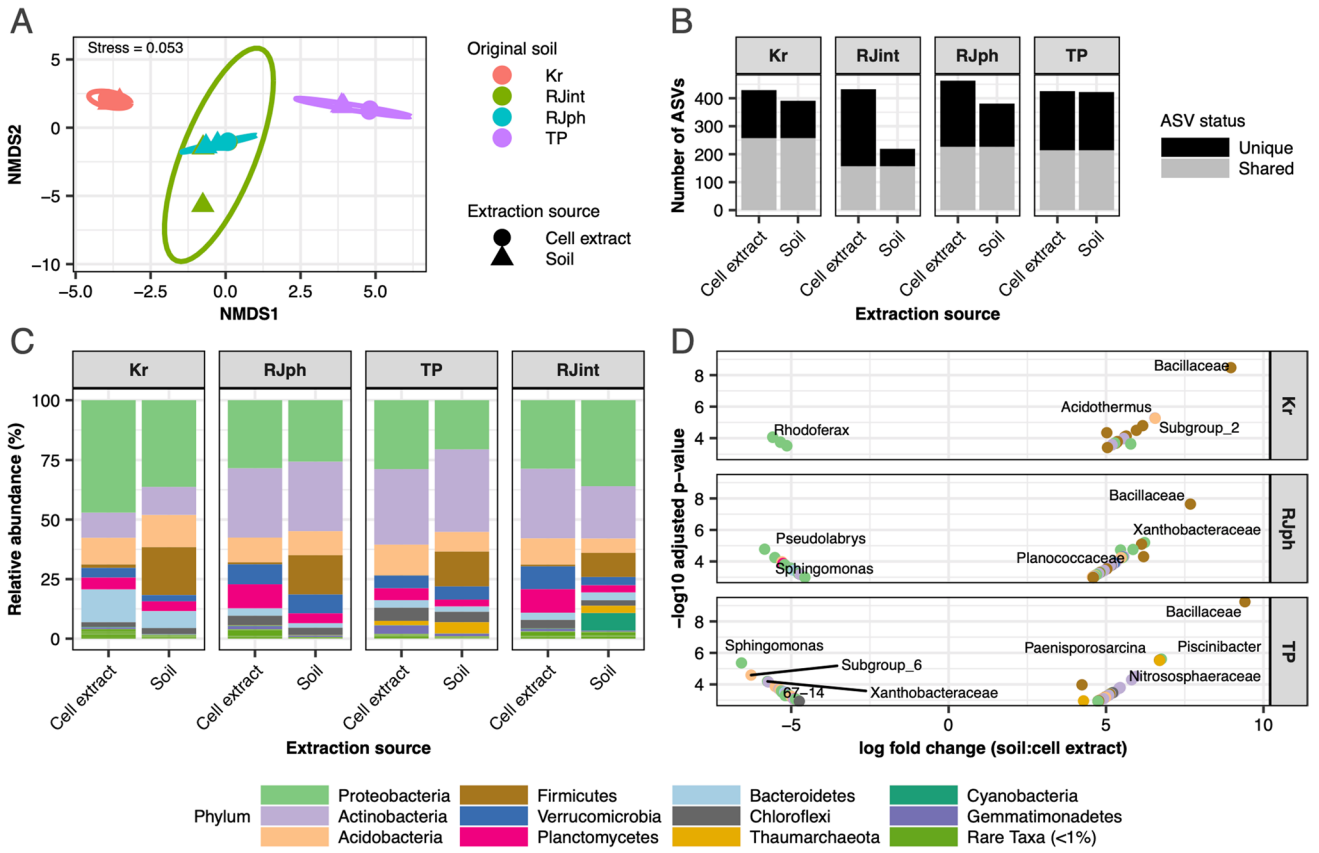

Fig. 6 Extraction bias in microbial communities. Community differences due to cell extraction are shown using NMDS (A), zeta-diversity (B), and community abundance (C, D). NMDS shows community dissimilarity (Bray–Curtis), where colors represent origin soil and shapes extraction source (soil or extracted cells). B depicts shared and unique ASVs between soil and cell extracted sequences. C depicts differences in phylum level relative abundance between soil and cell DNA extraction sources. D depicts fold changes in specific ASVs between soil and cell DNA extraction sources, calculated by dividing ASV abundance from soil communities, by those from extracted cells. ASVs with significant changes are labelled by genera

is unclear (Brenzinger et al. 2015; Dörsch et al. 2012; Nadeem et al. 2013).

2) Low N_2O accumulation and N_2O ratios during the early incubation period (Fig. S3, Fig. S4). As denitrification progressed following initial lag, most N-gas accumulation was as N_2. This occurred in the majority of CBA treatments, notably excluding those containing Tapawera cells, and resulted in lowered N_2O ratios relative to parent soils. Some previous cell-based studies also report very low N_2O production (Brenzinger et al. 2015; Dörsch et al. 2012). This may result from non-limiting C availability in contrast to higher N_2O ratio/low C availability seen in later periods of the present assay (see below).
3) A secondary period of high N_2O accumulation/reduced N_2 production rates in cell-based incubations. Evidence discussed below suggests this was most likely a result of C limitation and utilization of less energetically favourable C sources.

Relevance to the soils is further dependent on extracted bacteriomes accurately representing soil bacteriomes. During any soil cell extraction method, only a portion of soil cells are extracted (Lindahl and Bakken 1995), leaving the possibility for biases in composition of the community extracted, e.g., diversity differences (Holmsgaard et al. 2011) and N_2O emission potential differences (Nadeem et al. 2013). Our own investigations revealed high similarity between parent soil and extracted cell bacteriomes at a DNA level but with some clear biases against certain taxa, e.g., Firmicutes (Fig. 6A). Unfortunately, we are unable to completely confirm this DNA represented viable cells rather than dead or free floating DNA which passed through the cell extraction procedure. Further, our investigations consistently identified a high number of unique ASVs in extracted cells and total observed richness above that captured from soils. The reason for this is unlikely to be resolved without further empirical evidence but could

be due to the larger soil pool and concentration steps used for cell extraction vs. direct soil DNA extractions, movement of species out of rare biosphere in response to the cell extraction protocol disturbance, removal of DNA sorbing soil particles which otherwise can inhibit recovery of DNA during extraction (Paulin et al. 2013), dilution of soil PCR/sequencing inhibitors, or increased relative abundance of rarer species due to destruction of abundant organisms during cell extraction. Irrespective of the above limitations, the extracted bacteriomes from separate soils will with certainty represent distinct bacteriomes from one another, while the conserved relative ranking of N_2O ratios between soil and cell-based assays indicate representivity at a functional level (Fig. 2).

Proximal vs. bacteriome effects

Cell origin impacted both N_2O ratio and emissions (Table 1), indicating a strong role for bacteriome composition in mediating N_2O emission potential. Previous extracted cell-based studies support this claim (Dörsch et al. 2012; Liu et al. 2014; Nadeem et al. 2013) but have typically focused on understanding soil community responses to pH and provide little evaluation of overall impact of community differences compared to other chemical controls. In contrast, another soil-based study previously found minimal impact of distal control (implied bacteriome composition) on N_2O ratio but significant impact on total emissions (rate/enzyme activity) (Čuhel and Šimek 2011). Here, the directionless effect of cell origin on N_2O ratio and emissions across both CBAs were appreciable, on average only 21 and 37% lower than chemical effects. Therefore, bacteriome composition should be considered an important determinant of N_2O emission potential.

Directional analyses (i.e., LE cells and extracts are expected to decrease N_2O emission potential and HE cells/extracts vice versa) supported the notion that specific bacteriomes and chemical backgrounds can be predictably generalized as lower or higher emitting. In the absence of pH effects (CBA-int or CBA-pH at pH 6.6), LE cells and extracts predictably lowered total emissions and ratios while HE cells and extracts increased them (Table 1, Table S2). Excepting a single case in which HE extracts increased total emissions due to an increased denitrification rate (Table S2, LE cells + HE extract). Such communities or chemical backgrounds might hypothetically be selected for in farm soils to reduce N_2O emissions. Generalizations might also be applied about the relative importance of bacteriome vs. chemical backgrounds. In the absence of pH effects (CBA-int or CBA-pH at pH 6.6), cell and extracts had a similar average impact on N_2O ratios but water extracts had a greater impact on total emissions due to effects on total estimated denitrification rates (Table 1, Table S2).

Contrastingly, our assays also supported specific less predictable interactions between certain cells, chemical backgrounds and pH that broke the above generalizations. Tapawera LE cells were particularly sensitive to lower pH (Table 2) and especially so in the HE chemical background, showing the highest N_2O ratios and total emissions of any treatment (Table 1, CBA-pH). Our ultimate interpretation is that some generalisations can be made about what is a "good" (low N_2O emitting) bacterial denitrifying community and chemical background but that unpredictable specific effects may occur, especially when cells are denitrifying below their typical pH.

An important caveat of all the above interpretations is our inability to completely confirm that cell origin effects were only the result of community composition effects. Extracted cells clearly displayed some lesser but notable activity when incubated in just H_2O (Fig. S3C, Fig. S4C) indicating some C pool associated with the cells (lysed cells, adherent C, stored C, catabolism of cell constituents). Differences in this C availability between different cell extractions could potentially influence the denitrification kinetics within the main treatments, especially rates. Cell + H_2O controls demonstrate similar gas accumulation rates across both cell types in CBA-int (Fig. S3C) indicating that, most likely, cell associated C should have little observable impact on treatment differences. However, this cannot be claimed for CBA-pH where gas accumulation rates were clearly lower in HE cell + H_2O controls (Fig. S4C).

pH effects

pH differences of just 0.6 points accounted for similar changes in N_2O ratio as differences in water extracts during CBA-pH (Fig. 4A). This is consistent with denitrification literature which commonly identifies pH as a major driving factor of differences in N_2O/N_2 emission ratios between soils (Čuhel and Šimek 2011; Liu et al. 2014; Šimek and Cooper 2002). In contrast, N_2O emissions were much less susceptible to pH change compared with water extract origin due to the conflicting effects of pH on N_2O ratio and total denitrification rates, which are also previously noted (Šimek et al. 2002). In one case, increasing the pH actually resulted in increased N_2O emissions. The present assays were carried out over a fixed time period so increased total denitrification rates resulted in greater hypothetical N_2O emissions. In vivo, as long as N_2O ratios are maintained, increases in total denitrification rate may simply decrease the time taken to process available N rather than increase emissions. However, N_2O emissions might be increased indirectly in this fashion by preventing N consumption by non-N_2O producing process e.g. DNRA, N-assimilation, Anammox. Therefore, this evidence supports the view that pH manipulation of soil is not necessarily a successful approach to reduce overall N_2O emissions as illustrated in previous studies (Jha et al. 2020). Further, we noted the unideal scenario in which decreasing

the pH experienced by higher pH adapted cells significantly increased the N_2O ratio, while increasing the pH experienced by lower pH adapted cells resulted in only a minor decrease of the N_2O ratio. In essence, it may be easier for pH change to cause detrimental effects than repair them. Although our pH system may not be ideal to test this effect. Due to the buffer system used, the low pH soil was already above its natural pH under the low pH treatment.

Differential stages in N_2O production: the role of carbon

The timing of sudden decreases in CO_2 production and overall denitrification rates (Fig. S2), combined with the lack of late N_2O accumulation from glutamate amended controls (Fig. 5) suggest C limitation caused the increased N_2O accumulation and reduced N_2 rate observed in the later period of the cell-based incubations. If simple C limitation was occurring, it is expected that drops in CO_2 production and denitrification rates would wane gradually over time as C concentrations reduced; however, the drops in CO_2 and denitrification rates were often well defined and rapid. Therefore, we suggest the sudden transitions in rates are the result of exhaustion of a more labile C pool and initiation, or maintenance, of consumption of a more recalcitrant C pool. Soil extracted C is typically quantified in these two separate pools with separate consumption rate constants assigned to the consumption of each pool (e.g., Bowen et al. 2009; Guigue et al. 2014; Kalbitz et al. 2003). The multiple (greater than two) N_2 rate switches observable in some incubations (Fig. S3A, LEC + HEE; Fig. S6, 6 LEC + LEE extended) suggest effects to denitrification rates could be through greater than two distinct C pools of consecutively reduced energy availability.

Alternatively, denitrification rates may be sustained by consumption of energy storage molecules or dead cell constituents during the reduced N_2 rate period. Increased N_2O accumulation was previously shown in monocultures of *Alcaligenes faecalis* during C limitation and co-occurred with consumption of energy storage molecules (Schalk-Otte et al. 2000). This was attributed to competition for limited electrons between N_2O reductase and the previous denitrification reductases. Under this mechanism, differing N-reductase electron carrier affinities or regulatory mechanisms create an uneven distribution of electrons to the separate denitrification steps (Pan et al. 2013; Ribera-Guardia et al. 2014; Schalk-Otte et al. 2000; Wang et al. 2018). Earlier N-reductases are thought to outcompete N_2O reductase resulting in N_2O accumulation during limited electron supply.

Electron competition is consistent with concurrent drops in CO_2 production, estimated total denitrification rates and uneven rebalancing of N_2O production/reduction in the present study, whether this is during consumption of energy storage molecules or more recalcitrant C. However, it is unclear how this mechanism should proceed in a complex community of denitrifiers as competition for electrons is only possible when N_2O production and reduction proceed within the same organism. This is not necessarily a valid assumption in a complex denitrifying community where multiple species of denitrifiers could specialize in separate steps of the process due to the modularity of denitrification genes (Graf et al. 2014; Lycus et al. 2017; Roco et al. 2017). Electron competition between N-reductases has been tested in complex communities (Pan et al. 2013; Ribera-Guardia et al. 2014; Wang et al. 2018), and in some cases, it was assumed that denitrification was carried out by complete denitrifiers based on the genera of the dominant microbes within the culture (Pan et al. 2013; Wang et al. 2018). In-depth sequencing of metagenomes and metatranscriptomes with genome reconstruction would be necessary to actually resolve the modularity of active denitrifiers within the present system since phylogeny is usually considered a poor predictor of denitrification genetic potential (Jones et al. 2008).

A point of confusion, possibly contradicting the above interpretations, is that cell + H_2O treatments also demonstrated the distinct denitrification rate changes which we have attributed to C limitation (Fig. S3C, Fig. S4C). This either means the C limitation hypothesis and associated interpretations are wrong or that these incubations began with a non or initially less limiting availability of C. Cells were washed multiple times during extraction to remove C from the suspension solution. It is therefore most likely that the utilized C sources in these treatments are derived from lysed cellular constituents, cell adherent C, insoluble C, or stored C.

Conclusion

These investigations provide causal evidence for bacteriome composition effects on N_2O emission potential, but these were on average still weaker than chemical effects. Differences in cell-based assay gas accumulation kinetics reduce the general applicability of this system to soils but also serendipitously provide evidence that C limitation or switching to more recalcitrant C sources can lead to increased N_2O emissions. Investigations into the effects of pH corroborate the large body of research, suggesting that this is a particularly important determinant of soil N_2O emission ratios but also suggest that its impact on total N_2O emissions could be minor compared to other soil variables. Ultimately, we add to the mounting evidence that bacteriome composition needs to be considered during soil manipulations aimed at reducing N_2O emissions. Future

studies using this experimental system should focus on profiling of soil water extracts for compounds potentially impacting N_2O reduction, e.g., Cu, different C compounds. The soil extracted bacteriomes may also provide a greater opportunity for high quality RNA extraction and associated downstream analyses.

Supplementary Information The online version contains supplementary material available at https://doi.org/10.1007/s00374-022-01690-5.

Author contribution MPH, LRB, PD, and SEM designed this study. MPH performed the experiment, collected and analyzed the data, and wrote the manuscript. LM helped with the gas analysis. ST helped with the bacteriome analysis. All authors reviewed and edited the manuscript and agreed to the published version of the manuscript.

Funding Open Access funding enabled and organized by CAUL and its Member Institutions. This work was funded by the New Zealand Government through the New Zealand Fund for Global Partnerships in Livestock Emissions Research to support the objectives of the Livestock Research Group of the Global Research Alliance on Agricultural Greenhouse Gases (Agreement number: 16084 and SOW12-GPLER-OU-SM) awarded to SEM and the University of Otago, New Zealand. MH was funded by a University of Otago Postgraduate Scholarship. PD received funding from the FACCE-ERA-GAS project MAGGE-pH under the grant agreement no. 696356.

Data availability Sequences are available in the NCBI Sequence Read Archive under BioProject ID PRJNA678002.

Declarations

Ethics approval Not applicable.

Conflict of interest The authors declare no competing interests.

References

Bouwman AF, Beusen AHW, Griffioen J, van Groenigen JW, Hefting MM, Oenema O, van Puijenbroek PJTM, Seitzinger S, Slomp CP, Stehfest E (2013) Global trends and uncertainties in terrestrial denitrification and N_2O emissions. Philos Trans R Soc B Biol Sci 368:20130112

Bowen SR, Gregorich EG, Hopkins DW (2009) Biochemical properties and biodegradation of dissolved organic matter from soils. Biol Fertil Soils 45:733–742

Braman RS, Hendrix SA (1989) Nanogram nitrite and nitrate determination in environmental and biological materials by vanadium (III) reduction with chemiluminescence detection. Anal Chem 61:2715–2718

Brenzinger K, Dörsch P, Braker G (2015) pH-driven shifts in overall and transcriptionally active denitrifiers control gaseous product stoichiometry in growth experiments with extracted bacteria from soil. Front Microbiol 6:961

Callahan BJ, McMurdie PJ, Rosen MJ, Han AW, Johnson AJA, Holmes SP (2016) DADA2: High-resolution sample inference from Illumina amplicon data. Nat Methods 13:581–583

Caporaso JG, Lauber CL, Walters WA, Berg-Lyons D, Huntley J, Fierer N, Owens SM, Betley J, Fraser L, Bauer M, Gormley N, Gilbert JA, Smith G, Knight R (2012) Ultra-high-throughput microbial community analysis on the Illumina HiSeq and MiSeq platforms. ISME J 6:1621–1624

Cavigelli MA, Robertson GP (2000) The functional significance of denitrifier community composition in a terrestrial ecosystem. Ecol 81:1402–1414

Čuhel J, Šimek M (2011) Proximal and distal control by pH of denitrification rate in a pasture soil. Agric Ecosyst Environ 141:230–233

Čuhel J, Šimek M, Laughlin RJ, Bru D, Chèneby D, Watson CJ, Philippot L, Cuhel J, Simek M, Laughlin RJ, Bru D, Cheneby D, Watson CJ, Philippot L (2010) Insights into the effect of soil pH on N_2O and N_2 emissions and denitrifier community size and activity. Appl Environ Microbiol 76:1870–1878

Dixon P (2003) VEGAN, a package of R functions for community ecology. J Veg Sci 14:927–930

Dörsch P, Braker G, Bakken LR (2012) Community-specific pH response of denitrification: experiments with cells extracted from organic soils. FEMS Microbiol Ecol 79:530–541

Firestone MK, Smith MS, Firestone RB, Tiedje JM (1979) The influence of nitrate, nitrite, and oxygen on the composition of the gaseous products of denitrification in soil. Soil Sci Soc Am J 43:1140

Ginestet C (2011) ggplot2: elegant graphics for data analysis. J R Stat Soc Ser A (Statistics Soc 174:245–246

Graf DRH, Jones CM, Hallin S (2014) Intergenomic comparisons highlight modularity of the denitrification pathway and underpin the importance of community structure for N2O emissions De Crécy-Lagard V (ed). PLoS One 9:e114118

Guigue J, Mathieu O, Lévêque J, Mounier S, Laffont R, Maron PA, Navarro N, Chateau C, Amiotte-Suchet P, Lucas Y (2014) A comparison of extraction procedures for water-extractable organic matter in soils. Eur J Soil Sci 65:520–530

Highton MP, Bakken LR, Dörsch P, Wakelin S, de Klein CAM, Molstad L, Morales SE (2020) Soil N2O emission potential falls along a denitrification phenotype gradient linked to differences in microbiome, rainfall and carbon availability. Soil Biol Biochem 150:108004

Holmsgaard PN, Norman A, Hede SCHR, Poulsen PHB, Al-Soud WA, Hansen LH, Sørensen SJ (2011) Bias in bacterial diversity as a result of Nycodenz extraction from bulk soil. Soil Biol Biochem 43:2152–2159

Holtan-Hartwig L, Dörsch P, Bakken LR (2000) Comparison of denitrifying communities in organic soils: kinetics of NO_3- and N_2O reduction. Soil Biol Biochem 32:833–843

Hope RM (2013) Rmisc: Ryan Miscellaneous R package version 1.5. https://cran.r-project.org/package=Rmisc

Intergovernmental Panel on Climate Change (2013) Climate change 2013 the physical science basis: Working Group I contribution to the fifth assessment report of the intergovernmental panel on climate change. Cambridge University Press, Cambridge, UK

Jha N, Palmada T, Berben P, Saggar S, Luo J, McMillan AMS (2020). Influence of liming-induced pH changes on nitrous oxide emission, nirS, nirK and nosZ gene abundance from applied cattle urine in allophanic and fluvial grazed pasture soils. Biol Fertil Soils: 811–824.

Jones CM, Stres B, Rosenquist M, Hallin S (2008) Phylogenetic analysis of nitrite, nitric oxide, and nitrous oxide respiratory

enzymes reveal a complex evolutionary history for denitrification. Mol Biol Evol 25:1955–1966
Jones CM, Spor A, Brennan FP, Breuil M-C, Bru D, Lemanceau P, Griffiths B, Hallin S, Philippot L (2014) Recently identified microbial guild mediates soil N_2O sink capacity. Nat Clim Chang 4:801–805
Kalbitz K, Schmerwitz J, Schwesig D, Matzner E (2003) Biodegradation of soil-derived dissolved organic matter as related to its properties. Geoderma 113:273–291
Kassambara A. (2020). 'ggpubr': 'ggplot2' Based Publication Ready Plots. R Packag version 025. https://rpkgs.datanovia.com/ggpubr/ (Accessed June 1, 2020).
Lim NYN, Frostegård Å, Bakken LR (2018) Nitrite kinetics during anoxia: the role of abiotic reactions versus microbial reduction. Soil Biol Biochem 119:203–209
Lindahl V, Bakken LR (1995) Evaluation of methods for extraction of bacteria from soil. FEMS Microbiol Ecol 16:135–142
Liu B, Frostegård Å, Bakken LR (2014) Impaired reduction of N2O to N2 in acid soils is due to a posttranscriptional interference with the expression of nosZ Bailey M (ed). MBio 5:e01383-14
Lycus P, Bøthun KL, Bergaust L, Shapleigh JP, Bakken LR, Frostegård Å (2017) Phenotypic and genotypic richness of denitrifiers revealed by a novel isolation strategy. ISME J 11:2219–2232
McMurdie PJ, Holmes S (2013) phyloseq: an R package for reproducible interactive analysis and graphics of microbiome census data. PLoS One 8:e61217
Molstad L, Dörsch P, Bakken LR (2007) Robotized incubation system for monitoring gases (O_2, NO, N_2O N_2) in denitrifying cultures. J Microbiol Methods 71:202–211
Molstad L, Dörsch P, Bakken L (2016) Improved robotized incubation system for gas kinetics in batch cultures. ResearchGate.
Morales SE, Cosart T, Holben WE (2010) Bacterial gene abundances as indicators of greenhouse gas emission in soils. ISME J 4:799–808
Nadeem S, Almås ÅR, Dörsch P, Bakken LR (2013) Sequential extraction of denitrifying organisms from soils; strongly attached cells produce less N_2O than loosely attached cells. Soil Biol Biochem 67:62–69
Noble R, Fuhrman J (1998) Use of SYBR Green I for rapid epifluorescence counts of marine viruses and bacteria. Aquat Microb Ecol 14:113–118
Pan Y, Ni B-J, Bond PL, Ye L, Yuan Z (2013) Electron competition among nitrogen oxides reduction during methanol-utilizing denitrification in wastewater treatment. Water Res 47:3273–3281
Paulin MM, Nicolaisen MH, Jacobsen CS, Gimsing AL, Sørensen J, Bælum J (2013) Improving Griffith's protocol for co-extraction of microbial DNA and RNA in adsorptive soils. Soil Biol Biochem 63:37–49
Philippot L, Čuhel J, Saby NPA, Chèneby D, Chroňáková A, Bru D, Arrouays D, Martin-Laurent F, Šimek M (2009) Mapping field-scale spatial patterns of size and activity of the denitrifier community. Environ Microbiol 11:1518–1526
Quast C, Pruesse E, Yilmaz P, Gerken J, Schweer T, Yarza P, Peplies J, Glöckner FO (2013) The SILVA ribosomal RNA gene database project: improved data processing and web-based tools. Nucleic Acids Res 41:D590–D596
R Core Team (2016) R: A language and environment for statistical computing. R Foundation for Statistical Computing, Vienna, Austria. https://www.r-project.org/
Ribera-Guardia A, Kassotaki E, Gutierrez O, Pijuan M (2014) Effect of carbon source and competition for electrons on nitrous oxide reduction in a mixed denitrifying microbial community. Process Biochem 49:2228–2234
Robinson MD, McCarthy DJ, Smyth GK (2009) edgeR: a Bioconductor package for differential expression analysis of digital gene expression data. Bioinforma. https://doi.org/10.1093/bioinformatics/btp616
Roco CA, Bergaust LL, Bakken LR, Yavitt JB, Shapleigh JP (2017) Modularity of nitrogen-oxide reducing soil bacteria: linking phenotype to genotype. Environ Microbiol 19:2507–2519
Samad MS, Biswas A, Bakken LR, Clough TJ, de Klein CAM, Richards KG, Lanigan GJ, Morales SE (2016) Phylogenetic and functional potential links pH and N_2O emissions in pasture soils. Sci Rep 6:35990
Schalk-Otte S, Seviour R, Kuenen J, Jetten MS (2000) Nitrous oxide (N_2O) production by Alcaligenes faecalis during feast and famine regimes. Water Res 34:2080–2088
Šimek M, Cooper JE (2002) The influence of pH on denitrification: progress towards the understanding of this interaction over the last fifty years. Eur J Soil Sci 53:345–354
Šimek M, Jíšová L, Hopkins DW (2002) What is the so-called optimum pH for denitrification in soil? Soil Biol Biochem 34:1227–1234
Smith MS, Tiedje JM (1979) Phases of denitrification following oxygen depletion in soil. Soil Biol Biochem 11:261–267
Syakila A, Kroeze C (2011) The global nitrous oxide budget revisited. Greenh Gas Meas Manag 1:17–26
Wallenstein MD, Myrold DD, Firestone M, Voytek M (2006) Environmental controls on denitrifying communities and denitrification rates: insights from molecular methods. Ecol Appl 16:2143–2152
Wang Q, Garrity GM, Tiedje JM, Cole JR (2007) Naïve Bayesian classifier for rapid assignment of rRNA sequences into the new bacterial taxonomy. Appl Environ Microbiol 73:5261–5267
Wang Y, Li P, Zuo J, Gong Y, Wang S, Shi X, Zhang M (2018) Inhibition by free nitrous acid (FNA) and the electron competition of nitrite in nitrous oxide (N_2O) reduction during hydrogenotrophic denitrification. Chemosphere 213:1–10
Wickham H (2020) forcats: tools for working with categorical variables. R package version 0.5.0. https://cran.r-project.org/package=forcats
Wickham H, François R, Henry L, Müller K (2019) dplyr: a grammar of data manipulation. R package version 0.4.2. https://cran.r-project.org/package=dplyr
Zumft WG (1997) Cell biology and molecular basis of denitrification. Microbiol Mol Biol Rev 61:533–616